Dalton
Transactions

An international journal of inorganic chemistry

rsc.li/dalton

Volume 46
Number 10
14 March 2017
Pages 3073-3412

COMMUNICATION
Douglas W. Stephen et al
N-Heterocyclic carbene stabilized parent sulfenyl, selenenyl,
and tellurenyl cations (XH+; X = S, Se, Te)

ISSN 0306-0012

ROYAL SOCIETY
OF CHEMISTRY

This is an Accepted Manuscript, which has been through the Royal Society of Chemistry peer review process and has been accepted for publication.

Accepted Manuscripts are published online shortly after acceptance, before technical editing, formatting and proof reading. Using this free service, authors can make their results available to the community, in citable form, before we publish the edited article. We will replace this Accepted Manuscript with the edited and formatted Advance Article as soon as it is available.

You can find more information about Accepted Manuscripts in the Information for Authors.

Please note that technical editing may introduce minor changes to the text and/or graphics, which may alter content. The journal's standard Terms & Conditions and the Ethical guidelines still apply. In no event shall the Royal Society of Chemistry be held responsible for any errors or omissions in this Accepted Manuscript or any consequences arising from the use of any information it contains.

Dalton Transactions Accepted Manuscript

ARTICLE

Synthesis and characterisation of Co(III) complexes of *N*-formyl hydroxylamines and antibacterial activity of a Co(III) peptide deformylase inhibitor complex

Máté Kozsup,[a] Donal M. Keogan,[b] Deirdre Fitzgerald-Hughes,[c] Éva A. Enyedy,[d,e] Brendan Twamley,[f] Péter Buglyó[a] and Darren M. Griffith[b,g]*

The X-ray crystal structure and pK_a values of GSK322 a well-known and effective peptide deformylase inhibitor and antibacterial drug candidate are reported. The first examples of Co(III) complexes of *N*-formyl hydroxylamines are reported. Reaction of *N*-hydroxy-*N*-phenylformamide (HFA) with [Co(tren)Cl$_2$]Cl and [Co(tpa)Cl$_2$]Cl (where tren = tris(2-aminoethyl)amine, tpa = tris(2-pyridylmethyl)amine) with one equivalent of NaOH in H$_2$O afforded [Co(tren)(HFA$_{-1H}$)](PF$_6$)$_{1.5}$Cl$_{0.5}$ (**1**) and [Co(tpa)(HFA$_{-1H}$)]Cl$_2$ (**2**), respectively. X-ray crystal structures of both complexes revealed that the *N*-formyl hydroxylamine group acts as a bidentate ligand, coordinating the Co(III) centres via the carbonyl oxygen and deprotonated hydroxy group (*O,O'*), a coordination mode typically observed for closely related mono-deprotonated hydroxamic acids. Reaction of the *N*-formyl hydroxylamine-based GSK322 with [Co(tpa)Cl$_2$]Cl afforded the corresponding Co(III) chaperone complex of the peptide deformylase inhibitor, [Co(tpa)(GSK322$_{-1H}$)](PF$_6$)$_2$. GSK322 and [Co(tpa)(GSK322$_{-1H}$)](PF$_6$)$_2$ exhibited better Gram-positive activity than Gram-negative, where low MICs (1.56 – 6.25 μM) were determined for *S. aureus* strains, independent of their antibiotic susceptibility.

Introduction

The evolutionary pressure for the emergence of antibacterial resistance is significant due to the widespread use of antibiotics in human and veterinary medicine, agriculture and horticulture. In turn drug resistant infections represent an increasingly serious global health challenge and one of the greatest threats to human health.[1, 2]

Given that the prospect of untreatable bacterial infections is now becoming a reality, there is an urgent need to develop new classes of effective antibacterial agents.

Peptide deformylase (PDF), is an essential zinc based metalloenzyme which catalyses the removal of *N*-formyl groups from *N*-terminal methionine of newly synthesized bacterial polypeptides and represents an important unexploited target in antibacterial drug discovery.[3]

a. Department of Inorganic and Analytical Chemistry, University of Debrecen, H-4032 Debrecen, Egyetem tér 1, Hungary,
b. Department of Chemistry, Royal College of Surgeons in Ireland, 123 St. Stephens Green, Dublin 2, Ireland.
c. Department of Clinical Microbiology, Royal College of Surgeons in Ireland, RCSI Education & Research Centre, Beaumont Hospital, Beaumont, Dublin 9, Ireland.
d. Department of Inorganic and Analytical Chemistry, Interdisciplinary Excellence Centre, University of Szeged, Dóm tér 7, H-6720 Szeged, Hungary
e. MTA-SZTE Lendület Functional Metal Complexes Research Group, University of Szeged, Dóm tér 7, H-6720 Szeged, Hungary
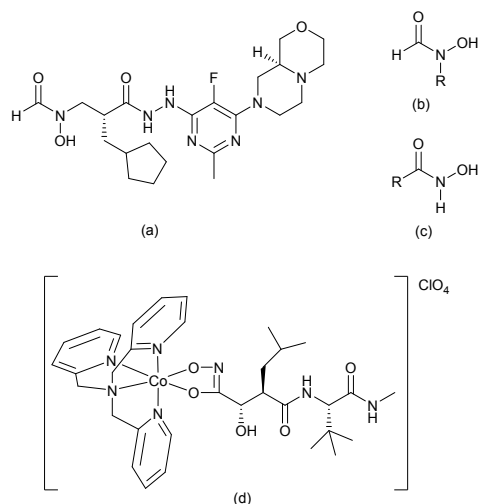f. School of Chemistry, Trinity College Dublin, University of Dublin, Dublin 2, Ireland.
g. SSPC, Synthesis and Solid State Pharmaceutical Centre, Ireland
*Fax: 353 1 402 2168 Tel: 353 1 402 2246, E-mail: dgriffith@rcsi.ie
Electronic Supplementary Information (ESI) available: [details of any supplementary information available should be included here]. See DOI: 10.1039/x0xx00000x

GSK1322322 (GSK322, *N*-((R)-2-(cyclopentylmethyl)-3-(2-(5-fluoro-6-((S)hexahydro- pyrazino[2,1-*c*][1,4]oxazin-8(1*H*)-yl)-2-methylpyrimidin-4yl)hydrazinyl)-3-oxopropyl)-*N*-hydroxy-formamide), Figure 1, is an *N*-formyl hydroxylamine-based potent and reversible inhibitor of PDF developed by GlaxoSmithKline (GSK).[4] *N*-formyl hydroxylamines are also known as reverse- or retro-hydroxamates and much like hydroxamic acids represent an important class of bidentate metal-chelating functional group, Figure 1.[5-8]

GSK322 exhibits good *in vitro* antibacterial activity against bacteria associated with acute bacterial skin and skin structure infections and community-acquired bacterial pneumonia. GSK322 exhibits no cross-resistance and is active against pathogenic strains resistant to commonly used antibacterial agents including β-lactams, macrolides, and quinolones.[4, 9, 10]

GSK322 can be deactivated *in vivo* through the formation of an *O*-glucuronide derivative which is pharmacologically inactive,[4] in much the same way that the hydroxamic acid functionalities are metabolised by glucuronidation.[11] Significantly GSK322 is currently no longer being developed by GSK due to "potentially reactive metabolites found in non-clinical studies, which created an unfavorable risk-benefit profile for a community agent (ClinicalTrials.gov registration no. NCT01818011)".[10]

Bioreductive cobalt(III) complexes, which possess for example cyclen, tris(2-pyridylmethyl)amine (tpa) or tris(2-aminoethyl)amine (tren) based tetradentate scaffolds, have been developed by Hambley and co-workers as chaperones for biologically active anticancer agents, including hydroxamic acid-based anticancer ligands, Figure 1 (d).[12] Such Co(III) complexes have reduction potentials in the biologically relevant window of

ARTICLE

Journal Name

-200 to -400 mV and are typically reduced to Co(II) under hypoxic conditions, which prevail in tumours, with concomitant release of bioligand of interest.[12]


Fig. 1. Structures of (a) PDF inhibitor GSK1322322, (b) *N*-formyl hydroxylamine (general), (c) hydroxamic acid (general), and (d) [Co(III)(Mar$_{-2H}$)(tpa)]ClO$_4$[12] where Mar$_{-2H}$ is the doubly deprotonated hydroximato form of Marimistat, a potent hydroxamic acid based matrix metalloproteinase inhibitor and anticancer agent.

Significantly hypoxia is also associated with wound tissue.[13] Three major factors are believed to primarily contribute to wound tissue hypoxia, which can range from near-anoxia to mild hypoxia; (i) peripheral arterial diseases limiting O$_2$ supply, (ii) greater O$_2$ demand of healing tissue and (iii) generation of reactive oxygen species (ROS) through respiratory burst and for redox signaling.[13]

Furthermore Co(III) chaperone complexes can also potentially protect sensitive bioligands against deactivation, minimise off-target binding and reduce toxic side effects.[12]

Recently Buglyó and co-workers developed a class of Co(III) chaperone complexes of the quinolones nalidixic acid (nalH) and its four fluoro derivatives, ciprofloxacin (cipH), norfloxacin (norH), sparfloxacin (spaH) and levofloxacin (levH) and reported relatively good antimicrobial activity against *E. coli* K-12 strain, with minimum inhibitory concentration (MIC) values in the μM range, Figure 2.[14]
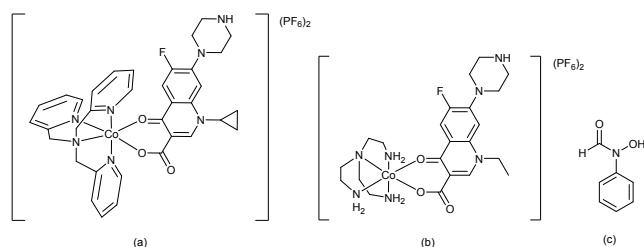
Fig. 2. Structures of (a) [Co(tpa)(cip)](PF$_6$)$_2$, (b) [Co(tren)(nor)](PF$_6$)$_2$ and (c) HFA.

We report herein an investigation of the reactivity of [Co(tren)Cl$_2$]Cl and [Co(tpa)Cl$_2$]Cl with *N*-hydroxy-*N*-

phenylformamide (HFA) to confirm coordination of the *N*-formyl hydroxylamine functionality and establish its coordination mode. Furthermore given the potential for Co(III) chaperone complexes to protect sensitive functional groups, reduce toxic side effects and to release bioactive ligands on reduction to Co(II) in hypoxic environments such as wound tissue we wished to develop a Co(III) chaperone complex for the potent PDF inhibitor GSK322.

Results and Discussion
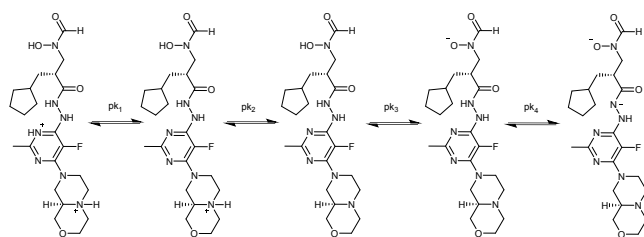
X-ray structure of GSK322

The previously unreported X-ray crystal structure of GSK322 was successfully solved upon growing single crystals under slow evaporation from a THF solution, Figure 3.
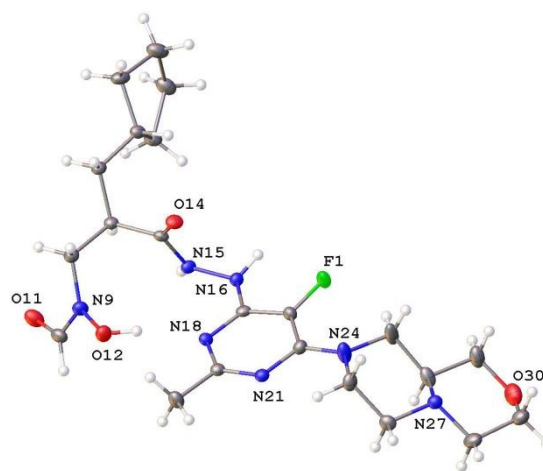
Fig. 3. Molecular structure of GSK322 (heteroatoms labelled only) without disordered THF solvate and with atomic displacement shown at 50% probability.

Solution studies of GSK322

The proton dissociation constant (pK_a) of a drug molecule is a key parameter since it affects the pharmacokinetic properties, and with the pK_a values the actual protonation state and charge can be calculated at a chosen pH. The proton dissociation processes of GSK322 were monitored by the combined use of pH-potentiometric, UV-visible (UV-vis) spectrophotometric and ^{1}H NMR titrations. The poor water solubility of the compound excluded performing pH-potentiometric studies in pure water; therefore a 30% (w/w) DMSO/H$_2$O solvent mixture was used for the measurements. The hydrolytic stability of the compound was investigated by consecutive pH-potentiometric titrations, which showed that no ligand decomposition occurred in the pH range studied (pH 2.0–12.5) under the argon atmosphere. The studied compound consists of four functional groups (pyrimidinium NH$^+$, oxazine NH$^+$, *N*-formyl hydroxylamine (HCONROH) and hydrazinic NH, Scheme 1) which presumably dissociate. pK_a values for all these deprotonation steps could be determined by the different methods (Table 1) under the applied conditions.

Scheme 1. Deprotonation steps of compound GSK322

Fig. 4. UV–vis spectra recorded for GSK32 at pH 2–12.5 (a). Individual calculated molar absorbance spectra of ligand species at various protonation states. {cL = 0.106 mM; l = 0.5 cm; 30% (w/w) DMSO/H2O; I = 0.1 M (KCl); T = 25 °C}

The obtained constants were in good agreement, although the magnitudes of the pK_1 and pK_4 values, fairly low and fairly high, respectively, hampered their accurate determination since these deprotonation steps take place in the pH-ranges where the pH measurements become uncertain. Notably the deprotonation processes are practically non-overlapping, and each pK_a can be attributed to a given moiety. Therefore, pK_1 is associated with deprotonation of the pyrimidinium nitrogen, pK_2 with the oxazine NH$^+$; while pK_3 and pK_4 can be attributed to the proton dissociation of the *N*-formyl hydroxylamine and the hydrazide groups, respectively (Scheme 1, Table 1). pK_a of the structurally related hydroxamic acid (Aha) was also determined for comparison under the same conditions and 9.89±0.01 was obtained. This value was markedly higher in the presence of DMSO than in pure water (pK_a = 9.26 in H$_2$O)[15] due to the deprotonation of a neutral functional group as it is expected on the basis of the Born electrostatic solvent model.[16] As it can be seen pK_3 of the *N*-formyl hydroxylamine group of GSK322 was one order of magnitude lower than pK_a of the Aha, similarly to the lower pK_a of formohydroxamic acid as well (pK_a = 8.65 in H$_2$O)[17] as a consequence of the presence of the electron donating methyl group in Aha.

The assignation of the pK_a values to the different functional groups was confirmed by analysis of the results of the UV–vis and ^{1}H NMR titrations. The UV–vis spectra recorded in the pH range from 2.0 to 12.5 (Figure 4a) show characteristic spectral changes at pH < ~4 and pH > ~10, while spectra display only minor alterations in the middle pH range. The molar absorbance spectra of the individual ligand species (H$_4$L^{2+}, H$_3$L$^+$, H$_2$L, HL$^-$, L^{2-}, Figure 4b) as well as the pK_a values (Table 1) were also calculated by the deconvolution of the pH-dependent UV–vis spectra recorded. Deprotonation of the oxazine NH$^+$ (pK_2: H$_3$L$^+$ → H$_2$L) and the *N*-formyl hydroxylamine group (pK_3: H$_2$L → HL$^-$) moieties are not expected to be accompanied by significant spectral changes since they are located relatively far from the chromophoric units, unlike pyrimidinium NH$^+$ (pK_1: H$_4$L^{2+} → H$_3$L$^+$) and the hydrazide NH (pK_4: HL$^-$ → L^{2-}). Therefore, individual molar absorbance spectra of H$_3$L$^+$, H$_2$L, HL$^-$ species show strong similarity (Figure 4b). It should be noted that the actual localization of the negative charge on the deprotonated hydrazide moiety is not known owing to the keto/enol tautomeric equilibrium.
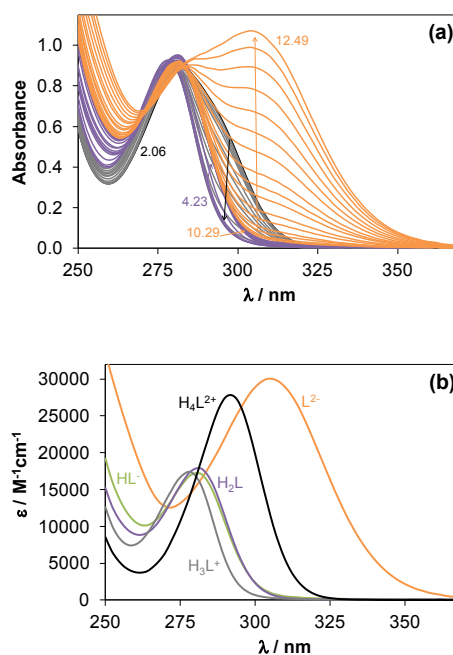
^{1}H NMR spectra recorded for GSK322 (Figure S1) show that certain proton resonances are sensitive to stepwise proton dissociation steps. Namely, the chemical shift (δ) of CH=O proton of the *N*-formyl hydroxylamine group revealed considerable changes only in the third deprotonation step when this moiety is losing the proton and was found to be insensitive to the other processes (Figures. S1 and 5c). On the other hand, all the deprotonation steps are accompanied by significant electronic shielding effect in the case of the protons of the methyl group at the pyrimidine ring (Figure 5b.); however the biggest change was observed according to the first deprotonation step. Only pK_1, pK_2 and pK_3 values could be determined based on the shift of the position of the CH=O and CH$_3$ protons with adequate accuracy which correspond well to those resulting from the other methods (Table 1). Representative concentration distribution curves calculated with the pK_a values determined by pH-potentiometry are shown in Figure 5a together with the pH-dependence of the chemical shifts of the CH=O and CH$_3$ protons (Figures. 5b,c).

On the whole, the results of the UV–vis and ^{1}H NMR titrations confirm the suggested sequence for the deprotonation steps (Scheme 1) and based on the determined pK_a values it can be concluded that GSK322 is mainly present in its neutral form at physiological pH (97 % H$_2$L).

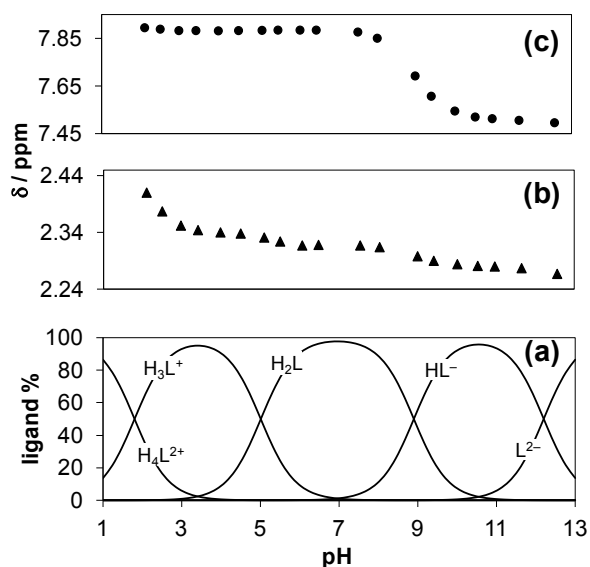**Fig. 5.** Concentration distribution curves of GSK322 calculated on the basis of the pKa values determined by pH-potentiometry (a). Chemical shifts of the methyl (▲) (b) and CH=O (●) (c) protons plotted against the pH. {cL = 0.96 mM; 30% (v/v) DMSO-d6/H2O; I = 0.1 M (KCl); T = 25 °C}

Table 1. Proton dissociation constants (pK_a) of GSK322 and Aha determined by pH-potentiometric, UV-vis spectrophotometric and ^{1}H NMR titrations. {30% (w/w) DMSO/H$_2$O; T = 25.0 °C; I = 0.20 M (KCl)}

ligand	method	pK_1	pK_2	pK_3	pK_4
GSK1322322	pH-metry	1.78	5.02	8.89	12.2
		±0.09	±0.03	±0.02	±0.1
	UV−vis	1.89	4.97	8.75	12.2
		±0.05	±0.02	±0.01	±0.1
	^{1}H NMR	1.8 ±0.1	5.07	8.96	>12
			±0.04	±0.01	
Aha	pH-metry	9.89	–	–	–
		±0.01[a]			

[a] pK_1 = 9.26 in water.[15]

Synthesis of cobalt complexes

Synthesis of cobalt complexes of HFA

HFA, was selected as a representative to investigate the reactivity of *N*-formyl hydroxylamines with Co(III) centres and establish resultant coordination mode(s). Reaction of equimolar equivalents of HFA with Co(III) chaperone precursor complexes, [Co(tren)Cl$_2$]Cl and [Co(tpa)Cl$_2$]Cl with a strong base in water afforded the corresponding complexes, [Co(tren)(HFA$_{-1H}$)](PF$_6$)$_{1.5}$Cl$_{0.5}$ (**1**) and [Co(tpa)(HFA$_{-1H}$)]Cl$_2$ (**2**), respectively. Both complexes were fully characterised by elemental analysis, IR and ^{1}H NMR spectroscopy, mass spectrometry and X-ray crystallography.

In regards to [Co(tren)(HFA$_{-1H}$)](PF$_6$)$_{1.5}$Cl$_{0.5}$.H$_2$O (**1**) and as a representative example, the elemental analysis was consistent with one singly deprotonated HFA ligand (HFA$_{-1H}$), one tren ligand, one and a half hexafluorophosphate and a half chloride per Co(III) centre. In the ^{1}H NMR spectra (D$_2$O, Figure S2) of **1** for example no signal associated with the *N*-formyl hydroxylamine hydroxyl group was observed as expected in D$_2$O

regardless of coordination. In **1** the most noteworthy shift as compared to the free HFA ligand is that of the formyl proton from 8.50 and to 7.77 ppm. The aromatic signals associated with the phenyl group are found as multiplets at 7.55 and 7.49 ppm integrating for 2 and 3 protons respectively. Previous ^{1}H NMR studies have highlighted that Co tren and tpa complexes bound to unsymmetrical bidentate ligands can exist as a mixture of two isomers in solution.[12] Consequently one might expect the presence of two isomer; *cis*- and *trans*- isomers, where the tripodal tertiary nitrogen is either *cis* or *trans* to the deprotonated *N*-hydroxy group of HFA$_{-1H}$ respectively.[12] Only one isomer was observed in the ^{1}H NMR spectra as evidenced by the presence of only one formyl H signal for example. Given the yield of **1** was low (20%) it is likely that the second isomer remained in the mother liquor and did not precipitate on the addition of NH$_4$PF$_6$.

The IR spectrum of **1** (Figure S3) exhibits distinctive ν(C=O) at 1627 cm^{-1} and the characteristic shift expected with bidentate (*O,O'*) *N*-formyl hydroxylamine coordination when compared to the corresponding ν(C=O) of the uncoordinated HFA ligand (1655 cm^{-1}).

ESI-MS in the positive mode (Figure S4) was used to identify the complex cation of **1**, [Co(tren)(HFA$_{-1H}$)]$^+$ (340.2). The analysis outlined for **1** is supported by X-ray crystallography. Single crystals of **1** were isolated from an ethanolic solution on slow evaporation, Figure 6.
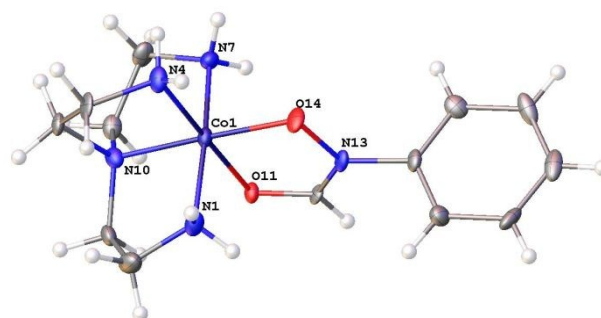

Fig. 6. Molecular structure of one independent octahedrally coordinated cation in **1** with heteroatoms labelled only. Anions, water and additional cation omitted (see Supporting Information for a full asymmetric unit).

In the crystal structure of **1** the deprotonated *N*-hydroxy group is observed to be *trans* to the tripodal tertiary amine of tren, Figures 6 and 7. A detailed description of the X-ray structure of **1** is provided in the supplementary material.

Interestingly in the ^{1}H NMR of **2** (D$_2$O, Figure S5) two geometric isomers were observed, likely the *cis*- and *trans*-isomers, Figure 7. Two formyl H signals were detected for example at 8.31 and 7.70 ppm in a 0.3:1 ratio.

The analysis outlined for **2** is also supported by X-ray crystallography. Single crystals of **2** were isolated from the concentrated mother liquor on standing, Figure 8.

In the crystal structure of **2** the deprotonated *N*-hydroxy group was also observed to be *trans* to the tripodal tertiary amine of tpa, Figures 7 and 8. A detailed description of the X-ray structure of **2** is provided in the supplementary material.
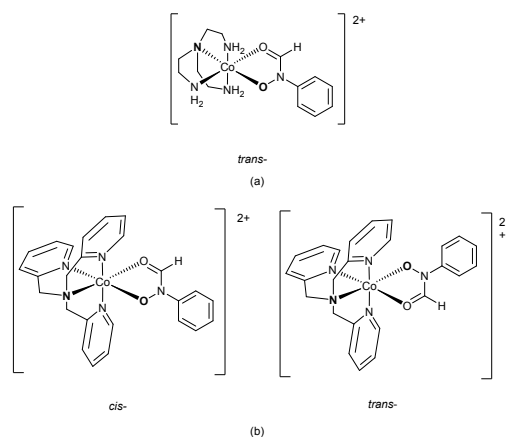
Fig. 7. Structures of Co HFA$_{-1H}$ complexes **1** as a *trans* isomer (a) and **2** as *cis*- and *trans*- isomers (b).
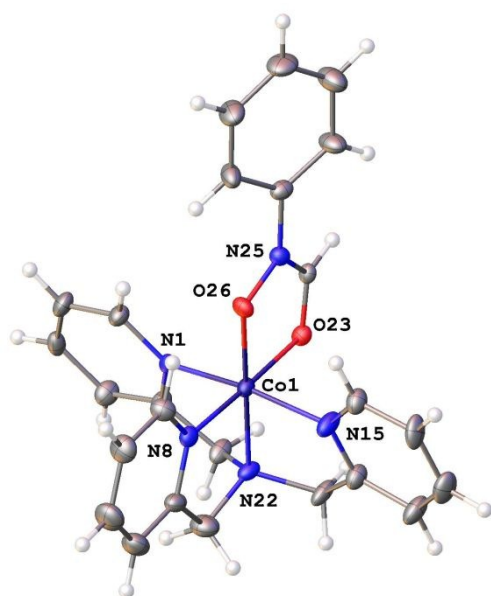

Fig. 8. Molecular structure of cation of **2**. Heteroatoms labelled only and water molecules and disordered chloride anions omitted for clarity. Displacement shown at 50% probability.

Synthesis of Co GSK322 complex

Reaction of equimolar equivalents of GSK322 with Co(III) chaperone precursor complex, [Co(tpa)Cl$_2$]Cl with a strong base in water afforded the corresponding complex, [Co(tpa)(GSK322$_{-1H}$)](PF$_6$)$_2$.2H$_2$O (**3,** Figure 9) in moderate yield. The complex was characterised by elemental analysis, IR and ^{1}H NMR spectroscopy and mass spectrometry. Elemental analysis is consistent with one GSK322 ligand per Co tpa complex.

In the ^{1}H NMR spectrum of the complex, signals associated with two isomers are also observed, suggesting in solution *cis* and *trans*- isomers co-exist in a 1:1 ratio. Signals are assigned in the experimental as being associated with isomer A or B, Figure S8. The likely challenging separation of the isomers was not attempted.

The IR spectrum of **3** (Figure S9) exhibited distinctive ν(C=O) at 1605 cm^{-1} and the characteristic shift expected with bidentate (O,O') *N*-formyl hydroxylamine coordination when compared to the corresponding ν(C=O) of the uncoordinated GSK322 ligand (1668 cm^{-1}).

HR-ESI-MS results in the positive mode (Figure S10) supports the proposed structure for **3** (Figure 9); m/z: 413.6713 [Co(tpa)(GSK$_{-1H}$)]$^{2+}$, 826.3354 [Co(tpa)(GSK$_{-1H}$)]-H]$^+$, 972.3074 ([Co(tpa)(GSK$_{-1H}$)](PF$_6$))$^+$.

An ^{1}H NMR stability study revealed that [Co(tpa)(GSK$_{-1H}$)](PF$_6$)$_2$ is stable in D$_2$O for at least 24 h, Figure S11. However, the stability of [Co(tpa)(GSK$_{-1H}$)](PF$_6$)$_2$ was not investigated in biological environments.
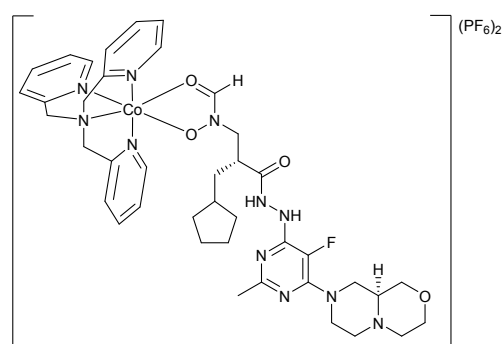
Fig. 9. Proposed structure of [Co(tpa)(GSK$_{-1H}$)](PF$_6$)$_2$, (**3**) (trans isomer).

Antibacterial activity

MIC values determined for each compound are shown in Table 2. The MIC value is defined as the lowest concentration of compound that inhibits the growth of the organism. Therefore the lower this value, the more potent the compound. HFA, a representative *N*-formyl hydroxylamine and its Co complexes **1** and **2** as expected exhibited no observable antibacterial activity with MICs greater than the highest concentration tested (200 µM).

In comparison, GSK322 had lower MIC values, indicating better antimicrobial activity in a similar range to those found for its Co(III) complex **3**.

GSK322 has been previuosly shown to be a narrow spectrum Gram-positive agent.[8, 9] Here GSK322 and its corresponding Co(III) PDF inhibitor complex and Co(III) chaperone candidate **3** demonstrated better Gram-positive activity than Gram-negative, where low MICs (1.56 and 6.25 µM) were determined for *S. aureus* strains, independent of their antibiotic susceptibility phenotype. GSK322 in particular demonstrated more potent activity against the MRSA strain (MIC = 1.56 µM) compared to ciprofloxacin (MIC = 25 µM), a broad spectrum antibiotic. Significantly **3** was twice as active than GSK322 against *S. aureus* 25923.

Given HFA and Co(III) HFA complexes **1** and **2** exhibited no discernable activity it is highly likely that the activity exhibited by **3** is associated with the release of GSK322 as a ligand. However, an investigation of the activity of **3** in the presence of known reductants was not undertaken.

ARTICLE

Journal Name

Table 2. MIC values (μM) for compounds against *S. aureus* and *E. coli* strains/isolates.

Bacteria	*	HFA	1	2	3	GSK 322	Ciprofloxacin
E. coli ATCC 25922	S	> 200	> 200	> 200	100	50	3.125
E.coli CL2 [a]	R	> 200	> 200	> 200	200	100	25
S. aureus ATCC 25923	S	> 200	> 200	> 200	3.125	6.25	3.125
S. aureus ATCC 43300	R	> 200	> 200	> 200	3.125	1.56	25

*S and R indicate antibiotic susceptible or resistant respectively. [a] multi-drug resistant due to production of extended-spectrum beta-lactamases, [b] MRSA strain, multi-drug resistant due to multiple mechanisms including alternative transpeptidase production. MIC values were determined in duplicate on at least three occasions. Where concentration following dilution reached more than three decimal places, they were rounded to two decimal places (eg 1.5625 to 1.56). Where no growth inhibiton was observed even at the maximum concentration tested, MIC was recorded as > 200 μM.

Conclusions

The previously unreported X-ray crystal structure of the potent PDF inhibitor GSK322 was reported. pK_a values determined for GSK322 by pH-potentiometry, UV-vis and ^{1}H NMR titrations revealed the deprotonation order of pyrimidinium nitrogen, oxazine NH[+]; hydroxamic acid and the hydrazide groups; and it could be concluded that the neutral form of the compound predominates at physiological pH. The first examples of Co(III) *N*-formyl hydroxylamines complexes are reported; [Co(tren)(HFA$_{-1H}$)](PF$_6$)$_{1.5}$Cl$_{0.5}$, [Co(tpa)(HFA$_{-1H}$)]Cl$_2$ and [Co(tpa)(GSK322$_{-1H}$)](PF$_6$)$_2$. X-ray crystal structures analyses reveal the *N*-formyl hydroxylamine group acts as a bidentate ligand, coordinating the Co(III) centres via the carbonyl oxygen and deprotonated hydroxy group (*O,O'*). GSK322 and the Co(III) chaperone PDF inhibitor complex, [Co(tpa)(GSK322$_{-1H}$)](PF$_6$)$_2$, a Co(III) chaperone candidate, demonstrated better Gram-positive activity than Gram-negative, where low MICs (1.56 – 6.25 μM) were determined for *S. aureus* strains, independent of their antibiotic susceptibility. GSK322 in particular demonstrated potent activity against the MRSA strain (MIC = 1.56 μM) in contrast to ciprofloxacin (MIC = 25 μM), a broad spectrum antibiotic. Significantly [Co(tpa)(GSK322$_{-1H}$)](PF$_6$)$_2$ was twice as active than GSK322 against *S. aureus* 25923.

Future work will be focused on investigating the activity of [Co(tpa)(GSK322$_{-1H}$)](PF$_6$)$_2$ in the presence of known reductants and in a range of environments that mimic wound infection.

Experimental

Materials and instrumentation

CoCl$_2$·6H$_2$O, NaNO$_2$, tris(2-aminoethyl)amine (tren) were used as received from Sigma Aldrich (Sigma Aldrich Ireland Ltd., Arklow, Co Wicklow). All other commercially available reagents and solvents, including deuterated solvents, were also purchased from Sigma-Aldrich and used without further purification. tpa,[18] HFA,[19] [Co(tren)Cl$_2$]Cl, [Co(tpa)Cl$_2$]Cl[20] were synthesized and purified as previously reported. GSK322 was generously gifted by GlaxoSmithKline (GSK, 1250 S. Collegeville Road, Collegeville, PA, USA). ^{1}H NMR and ^{13}C NMR spectra were recorded on a Bruker Avance 400 NMR spectrometer. The spectra were analysed using MestReNova software. The residual undeuterated solvent signals were used as internal references.[21] Mass spectrometry experiments were performed on an Advion Expression Compact Mass Spectrometer where 10 μL of the samples were injected in 300 μL of methanol:isopropanol:water:formic acid (80:10:10:1 v/v). The mass spectrometry data were acquired in positive ion mode and the spectra analysed using the Advion Mass Express software programme. Elemental analysis (C, H, N) was performed at the Microanalytical Laboratory, School of Chemistry and Chemical Biology, University College Dublin, Ireland.

Syntheses
[Co(tren)(HFA$_{-1H}$)](PF$_6$)$_{1.5}$Cl$_{0.5}$.0.33H$_2$O (1)
[Co(tren)Cl$_2$]Cl (100.00 mg, 0.32 mmol) and HFA (43.88 mg, 0.32 mmol) were dissolved in 20 mL water. NaOH (12.80 mg, 0.32 mmol) was added. The reaction mixture was stirred at 60 °C overnight, cooled and filtered. The filtrate was reduced to dryness *in vacuo*. The residue was dissolved in ethanol (20 mL) to which an ethanolic solution (20 mL) of NH$_4$PF$_6$ (104.32 mg, 0.64 mmol) was added. A purple solid precipitated on slow evaporation at RT. The solid was filtered and dried *in vacuo*. Yield: 40.17 mg (20 %).^{1}H NMR (400 MHz, D$_2$O): δ/ppm = 7.77 (s, 1H, Formyl H), 7.55 (m, 2H, ArH), 7.49 (m, 3H, ArH), 3.69 (m, 2H, -CH$_2$), 3.38 (m, 2H, -CH$_2$), 3.22 (m, 4H, -CH$_2$), 3.05 (m, 2H, -CH$_2$), 2.91 (t, 2H, -CH$_2$). IR (KBr)/cm^{-1}: 3330, 3117, 1628, 1463, 1320, 823, 770, 692, 554, 518. Anal. Required for C$_{13}$H$_{24.33}$Cl0.5CoF$_9$N$_5$O$_{2.165}$P$_{1.5}$: C, 26.95, H, 4.23, N, 12.09 %. Found: C, 26.57, H, 4.22, N, 11.83%. MS (ESI, positive ion): m/z: 340.2 ([Co(tren)(HFA$_{-H}$)]$^+$.
A single crystal of [Co(tren)(HFA$_{-H}$)](PF$_6$)$_{1.5}$Cl$_{0.5}$ was isolated on slow evaporation of an ethanolic solution.

[Co(tpa)(HFA$_{-1H}$)]Cl$_2$6.H$_2$O (2)
[Co(tpa)Cl$_2$]Cl (145.80 mg, 0.32 mmol) and HFA (43.88 mg, 0.32 mmol) were dissolved in 20 mL water to which NaOH (12.80 mg, 0.32 mmol) was added. The reaction mixture was stirred at 60 °C overnight. The mixture was filtered and the volume of the filtrate was reduced *in vacuo* to ca. 2 mL and subsequently stored at 4 °C for 24 h. A red crystalline solid was collected by filtration and dried *in vacuo*. Yield: 111.10 mg (39 %). ^{1}H NMR (400 MHz, D$_2$O): δ/ppm = 9.14 (d, 0.3H, ArH-isomer B) 8.85 (d, 1H, ArH-isomer A), 8.61 (d, 2H, ArH-isomer A), 8.35 (d, 0.6H, ArH-isomer B), 8.31 (s, 0.3H, Formyl H-isomer B), 7.96-7.92 (m, 2.6H, ArH-isomers A,B), 7.81-7.73 (m, 3.3H, ArH-iomers A,B), 7.70 (s, 1H, Formyl H-isomer A), 7.61-7.59 (m, 2.6H, ArH-isomers A,B), 7.56-7.40 (m, 6.8H, ArH-isomers A,B), 7.26-7.15

(m, 2.9H, ArH-isomers A,B) 5.51 (d, 2H, -CH$_2$-isomer A), 5.43 (d, 0.6H, -CH$_2$-isomer B), 5.12-5.03 (m, 4.6H, -CH$_2$-isomers A,B), 4.96 (d, 0.6H, -CH$_2$-isomer B). IR (KBr)/cm^{-1}: 3328, 1600, 1574, 1459, 1327, 886, 754. Anal. Required for C$_{25}$H$_{36}$Cl$_2$CoN$_5$O$_8$: C, 45.19, H, 5.46, N, 10.59. Found: C, 44.90, H, 560, N, 10.81%. MS (ESI, positive ion): m/z: 485.2 ([Co(tpa)(HFA$_{-H}$)]$^+$.

A single crystal suitable for X-ray Crystallography was isolated from the batch of crystalline solid.

[Co(tpa)(GSK322$_{-H}$)](PF$_6$)$_2$.2H$_2$O (3)

[Co(tpa)Cl$_2$]Cl (57.00 mg, 0.13 mmol) and GSK322 (60.00 mg, 0.13 mmol) were dissolved in 15 mL water. NaOH (5.00 mg, 0.13 mmol) was added. The reaction mixture was stirred at 60 ^{o}C for 6 h and at room temperature overnight. The mixture was concentrated to 5 mL *in vacuo* and 2 eq. of NH$_4$PF$_6$ (40.75 mg, 0.26 mmol) was added. A purple crystalline solid was filtered, washed with cold water and diethyl ether and dried *in vacuo*. Yield: 84.44 mg (60 %). ^{1}H NMR (400 MHz, D$_2$O): δ/ppm = 9.11 (d, 0.5H, ArH), 8.70 (d, 0.5H, ArH), 8.65 (d, 0.5H, ArH), 8.59 (d, 0.5H, ArH), 8.40 (d, 0.5H, ArH), 8.33 (d, 0.5H, ArH), 8.07 (t, 0.5H, ArH), 8.01 (t, 1H, ArH), 7.86 (m, 0.5H, ArH), 7.82 (m, 0.5H, ArH), 7.78 (m, 1H, ArH), 7.73 (m, 0.5H, ArH), 7.67 (m, 1H, ArH), 7.61-7.53 (m, 2H, ArH), 7.49 (m, 0.5H, ArH), 7.42 (m, 1H, ArH), 7.22 (m, 1H, ArH), 7.17 (m, 0.5H, ArH), 5.50 (m, 1H, -CH$_2$ tpa), 5.39 (m, 1H, -CH$_2$ tpa), 5.11-5.09 (m, 2.5H, -CH$_2$ tpa), 5.02 (m, 1H, -CH$_2$ tpa), 4.98 (m, 0.5H, -CH$_2$ tpa), 4.33-4.05 (m, 3H, -CH$_2$), 4.00-3.92 (m, 2H, -CH$_2$), 3.76 (m, 1H, -CH$_2$), 3.66-3.57 (m, 1H, -CH$_2$), 3.51-3.44 (m, 1.5H, -CH$_2$), 3.30-3.17 (m, 1H, -CH$_2$), 3.13-3.01 (m, 2H, -CH$_2$), 2.90-2.75 (m, 3.5H, -CH$_2$), 2.22 (s, 1.5H, -CH$_3$ isomer A), 1.96 (m, 1H, -CH$_2$), 1.88 (s, 1.5H, -CH$_3$ isomer B), 1.82-1.75 (m, 1.5H, -CH$_2$), 1.62-1.53 (m, 4H, -CH$_2$), 1.36 (m, 2.5H, -CH$_2$), 1.21 (m, 0.5H, -CH$_2$), 1.12 (m, 1H, -CH$_2$), 0.68 (m, 0.5H, -CH$_2$), 0.58 (m, 0.5H, -CH$_2$), 0.23 (m, 0.5H, -CH$_2$). IR (KBr)/cm^{-1}: 3404, 2947, 1605, 1451, 842, 558. Anal. Required for C$_{40}$H$_{55}$CoF$_{13}$N$_{11}$O$_6$P$_2$: C, 41.64, H, 4.80, N, 13.35 %. Found: C, 41.34, H, 4.86, N, 13.15 %. MS (ESI, positive ion): m/z: 413.6713 [Co(tpa)(GSK$_{-H}$)]$^{2+}$, 826.3354 [Co(tpa)(GSK$_{-H}$)-H]$^+$, 972.3074 ([Co(tpa)(GSK$_{-H}$)](PF$_6$)$^+$.

X-ray crystallographic measurements on GSK322, 2 and 3

Data was collected on a Bruker D8 Quest ECO using Mo Kα (λ = 0.71073 Å) radiation. Samples were mounted on a MiTeGen microloop and data collected at 100(2) K using an Oxford Instruments Cryostream low temperature device. Bruker APEX[22] software was used to collect and reduce data and determine the space group. Structures were solved with the XT structure solution program using Intrinsic Phasing and refined with the XL[23] refinement package using Least Squares minimisation with Olex2.[24] Absorption corrections were applied using SADABS or TWINABS.[25, 26] Crystal data, details of data collection and refinement are given in Table S1.

In GSK322, donor hydrogen atoms H15 and H16 were located and refined using restraints (DFIX). The THF solvent was modelled as disordered over two locations with occupancy 85:15 %. Restraints used (SIMU) for the disordered carbon atoms.

1 was refined as a three component rotational twin with BASF 0.0794(13); 0.1666(14); 0.1656(15), around the axes (100), (011) and (01-1). Cl1 was modelled as disordered over two locations with 80:20% occupancy. The hydrogen atoms on partially occupied (33%) O6 have been placed to optimize hydrogen bonding with Cl1 only. Restraints were used in the refinement (DFIX, ISOR).

2 was refined as a two component rotational twin. Rotated from first domain by 180.0 degrees about reciprocal axis 1.000 0.000 -0.280 and real axis 1.000 -0.001 0.004. Twin law to convert hkl from first to this domain (SHELXL TWIN matrix): 1.003 -0.001 0.009 0.001 -1.000 0.000 -0.561 0.000 -1.003. One chloride anion is disordered over 4 sites with occupancies 21:39:20:20% and was refined using restraints (SUMP, SIMU). One water molecule was refined with restraints (ISOR). Water hydrogen atoms were placed in ideal locations to ensure hydrogen bonding networks. Refined BASF = 0.1696(15).

CCDC 1992411-1992413 contain the supplementary crystallographic data for this paper. These data can be obtained free of charge from The Cambridge Crystallographic Data Centre via www.ccdc.cam.ac.uk/data_request/cif.

Solution equilibrium measurements and calculations

The pH-potentiometric measurements for the determination of the proton dissociation constants of GSK322 and acetohydroxamic acid (Aha) were carried out at 25.0 ± 0.1 ^{o}C in dimethyl sulfoxide (DMSO):water 30:70 (w/w) as solvent and at an ionic strength of 0.10 M (KCl). The titrations were performed with carbonate-free KOH solution of known concentration (0.10 M). The concentrations of the base and the HCl were determined by pH-potentiometric titrations. An Orion 710A pH-meter equipped with a Metrohm combined electrode (type 6.0234.100) and a Metrohm 665 Dosimat burette were used for the titrations. The electrode system was calibrated to the pH = −log[H$^+$] scale in the DMSO/water solvent mixture by means of blank titrations (strong acid *vs.* strong base: HCl *vs.* KOH), similarly to the method suggested by Irving *et al.*[27] The average water ionization constant pK_w was 14.52 ± 0.05, which corresponds well to the literature data.[28, 29] The reproducibility of the titration points included in the calculations was within 0.005 pH. The pH-metric titrations were performed in the pH range 2.0 – 12.5. The initial volume of the samples was 5.0 mL. The ligand concentration was 1.0 or 0.5 mM. Samples were deoxygenated by bubbling purified argon through them for approximately 10 min prior to the measurements. Argon was also passed over the solutions during the titrations. The exact concentration of the ligand stock solutions together with the proton dissociation constants were determined by pH-potentiometric titrations with the use of the computer program HYPERQUAD.[30]

A Hewlett Packard 8452A diode array spectrophotometer was used to record the UV–vis spectra in the 200 to 950 nm window. The path length was 0.5 cm. Proton dissociation constants of GSK322 and the molar absorbance spectra of the individual species were calculated with the computer program PSEQUAD.[31] The spectrophotometric titrations were performed on samples containing the GSK322 at 106 μM in the pH range

ARTICLE

Journal Name

from 2 to 12.5 at 25.0 ± 0.1 °C in DMSO:water 30:70 (w/w) at an ionic strength of 0.10 M (KCl).

^1H NMR spectroscopic titrations were carried out on a Bruker Ultrashield 500 Plus instrument. DSS was used as an internal NMR standard and WATERGATE method was used to suppress the solvent resonance. pH-dependency of the spectra of GSK322 was followed in a 30% (v/v) DMSO-d^6/H$_2$O mixture in a concentration of 0.96 mM at ionic strength of 0.10 M (KCl).

Bacterial cell culture

The following bacterial strains/isolates were tested; *Escherichia coli* strain ATCC25922 (antibiotic-susceptible), extended-spectrum beta lactamase (ESBL)-producing *E. coli* clinical isolate (CL2) recovered from a patient with a urinary tract infection, *Staphylococcus aureus* ATCC25923 (antibiotic susceptible) and a methicillin-resistant *S. aureus* (MRSA), ATCC 44330. All strains/isolates were grown routinely on Columbia Blood Agar (Cruinn Diagnostics, Ireland) with overnight incubation at 37°C, for isolation of single colonies.

MIC determination

MIC values were determined using the broth microdilution method according to the guidelines of the Clinical and Laboratory Standards Institute (CLSI). Suspensions of isolated colonies from each bacteria to be tested were prepared in Mueller Hinton Broth (non-cation adjusted, Oxoid, UK) and adjusted to the density of a 0.5 McFarland Standard using a Densichek Meter (Biomerieux, FR). This suspension was further diluted 1/50 (v/v) to approximately 3 x 10^6 colony forming units (CFU)/mL. Stock solutions of each compound were prepared at 2 mM in 2% DMSO and a serial doubling dilution was prepared from these (3.125 μM to 1 mM) in sterile deionized water. Assays were prepared in 96 wells plates where triplicate wells contained 10 µL of each concentration and 90 µL of diluted bacterial suspension. Plates were incubated at 37°C overnight in a static incubator. The MIC was recorded as the lowest concentration of compound showing no visible growth after approximately 18 h incubation with reference to positive growth control (no compounds) and negative controls (no bacteria).

Conflicts of interest
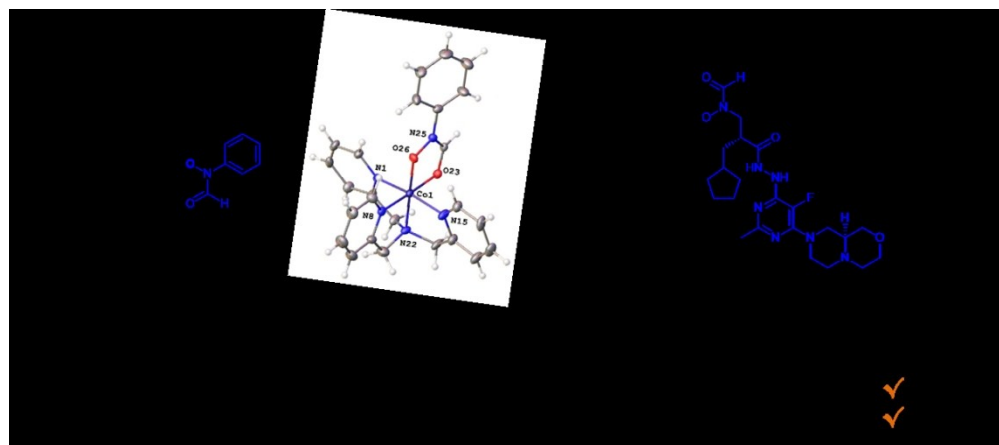
There are no conflicts to declare.

Acknowledgements

References

1. G. Barlow, *Nat. Microbiol.*, 2018, **3**, 258-260.
2. J. M. Blair, M. A. Webber, A. J. Baylay, D. O. Ogbolu and L. J. Piddock, *Nature reviews. Microbiology*, 2015, **13**, 42-51.
3. S. Fieulaine, R. Alves de Sousa, L. Maigre, K. Hamiche, M. Alimi, J.-M. Bolla, A. Taleb, A. Denis, J.-M. Pagès, I. Artaud, T. Meinnel and C. Giglione, *Sci. Rep.*, 2016, **6**, 35429.
4. D. Mamaril-Fishman, J. Zhu, M. Lin, C. Felgate, L. Jones, P. Stump, E. Pierre, C. Bowen, O. Naderer, E. Dumont, P. Patel, P. D. Gorycki, B. Wen, L. Chen and Y. Deng, *Drug Metab. Dispos.* , 2014, **42**, 1314-1325.
5. S. Price and S. E. Osbourn, *Org. Lett.*, 2005, **7**, 3761-3763.
6. D. M. Keogan, S. S. C. Oliveira, L. S. Sangenito, M. H. Branquinha, R. D. Jagoo, B. Twamley, A. L. S. Santos and D. M. Griffith, *Dalton Trans.*, 2018, **47**, 7245-7255.
7. D. M. Keogan, B. Twamley, D. Fitzgerald-Hughes and D. M. Griffith, *Dalton Trans.*, 2016, **45**, 11008-11014.
8. D. M. Griffith, M. Devocelle and C. J. Marmion, in *Amino Acids, Peptides and Proteins in Organic Chemistry*, ed. A. B. Hughes, 2010, DOI: 10.1002/9783527631780.ch3, pp. 93-144.
9. J. Hoover, T. Lewandowski, R. J. Straub, S. J. Novick, P. DeMarsh, K. Aubart, S. Rittenhouse and M. Zalacain, *Antimicrob Agents Chemother*, 2015, **60**, 180-189.
10. J. L. Hoover, C. M. Singley, P. Elefante, P. DeMarsh, M. Zalacain and S. Rittenhouse, *Antimicrob Agents Chemother*, 2017, **61**, e00959-00917.
11. P. Hermant, D. Bosc, C. Piveteau, R. Gealageas, B. Lam, C. Ronco, M. Roignant, H. Tolojanahary, L. Jean, P.-Y. Renard, M. Lemdani, M. Bourotte, A. Herledan, C. Bedart, A. Biela, F. Leroux, B. Deprez and R. Deprez-Poulain, *J. Med. Chem.*, 2017, **60**, 9067-9089.
12. B. P. Green, A. K. Renfrew, A. Glenister, P. Turner and T. W. Hambley, *Dalton Trans.*, 2017, **46**, 15897-15907.
13. C. K. Sen, *Wound Repair Regen*, 2009, **17**, 1-18.
14. M. Kozsup, E. Farkas, A. C. Bényei, J. Kasparkova, H. Crlikova, V. Brabec and P. Buglyó, *J. Inorg. Biochem.*, 2019, **193**, 94-105.
15. E. Farkas, E. Kozma, T. Kiss, I. Tóth and B. Kurzak, *J. Chem. Soc., Dalton Trans.*, 1995, DOI: 10.1039/DT9950000477, 477-481.
16. M. Born, *Z. Phys.*, 1920, **1**, 45-48.
17. E. P. Serjeant and B. Dempsey, *Ionisation constants of organic acids in aqueous solution*, Pergmon press, Oxford, 1979.
18. V. Chandrasekaran and S. J. Collier, in *Encyclopedia of Reagents for Organic Synthesis*, 2013, DOI: 10.1002/047084289X.rn01606.
19. J. R. Bourque, R. K. M. Burley and S. L. Bearne, *Bioorg. Med. Chem. Lett.*, 2007, **17**, 105-108.
20. E. Kimura, S. Young and J. P. Collman, *Inorg. Chem.*, 1970, **9**, 1183-1191.

Dalton Transactions

Journal Name

ARTICLE

21. H. E. Gottlieb, V. Kotlyar and A. Nudelman, *J. Org. Chem.*, 1997, **62**, 7512-7515.
22. Bruker, *Journal*, 2017.
23. G. M. Sheldrick, *Acta Crystallographica Section C: Structural Chemistry*, 2015, **71**, 3-8.
24. O. V. Dolomanov, L. J. Bourhis, R. J. Gildea, J. A. K. Howard and H. Puschmann, *Journal of Applied Crystallography*, 2009, **42**, 339-341.
25. Bruker, *Journal*, 2016.
26. G. M. Sheldrick, *Journal*, 2012.
27. H. M. Irving, M. G. Miles and L. D. Pettit, *Anal. Chim. Acta* 1967, **38**, 475–488.
28. É. A. Enyedy, O. Dömötör, E. Varga, T. Kiss, R. Trondl, C. G. Hartinger and B. K. Keppler, *J. Inorg. Biochem.*, 2012, **117**, 189-197.
29. *Journal*, 1993–2005.
30. P. Gans, A. Sabatini and A. Vacca, *Talanta*, 1996, **43**, 1739-1753.
31. L. Zékány and I. Nagypál, in *Computational Methods for the Determination of Stability Constants*, ed. D. L. Leggett, Plenum Press, New York, 1985, p. 291.

Dalton Transactions Accepted Manuscript

Bidentate *(O,O')* *N*-formylhydroxylamine chelation of Co(III) centres and notable antibacterial activity of a Co(III) peptide deformylase inhibitor complex against sensitive and resistant strains of *S. Aureus*

214x94mm (150 x 150 DPI)